Available online at www.sciencedirect.com
SCIENCE DIRECT®
Journal of Solid State Chemistry 178 (2005) 2376–2382
JOURNAL OF SOLID STATE CHEMISTRY
www.elsevier.com/locate/jssc

Inorganic–organic hybrid structure: Synthesis, structure and magnetic properties of a cobalt phosphite–oxalate, $[C_4N_2H_{12}][Co_4(HPO_3)_2(C_2O_4)_3]$

Sukhendu Mandal, Srinivasan Natarajan*

Framework Solids Laboratory, Solid State and Structural Chemistry Unit, Indian Institute of Science, Bangalore 560012, India

Received 28 March 2005; received in revised form 6 May 2005; accepted 20 May 2005

Abstract

A hydrothermal reaction of a mixture of cobalt (II) oxalate, phosphorous acid, piperazine and water at 150 °C for 96 h followed by heating at 180 °C for 24 h gave rise to a new inorganic–organic hybrid solid, $[C_4N_2H_{12}][Co_4(HPO_3)_2(C_2O_4)_3]$, I. The structure consists of edge-shared CoO_6 octahedra forming a $[Co_2O_{10}]$ dimers that are connected by HPO_3 and C_2O_4 units forming a three-dimensional structure with one-dimensional channels. The amine molecules are positioned within these channels. The oxalate units have a dual role of connecting within the plane of the layer as well as out of the plane. Magnetic susceptibility measurement shows the compound orders antiferromagnetically at low temperature ($T_N = 22\,K$). Crystal data: **I**, monoclinic, space group = $P2_1/c$ (No. 14). $a = 7.614(15)$, $b = 7.514(14)$, $c = 17.750(3)$ Å, $\beta = 97.351(3)^\circ$, $V = 1007.30(3)$ Å^3, $Z = 2$, $\rho_{calc} = 2.466\,g/cm^3$, $\mu_{(MoK\alpha)} = 3.496\,mm^{-1}$, $R_1 = 0.0310$ and $wR_2 = 0.0807$ data [$I > 2\sigma(I)$].

Keywords: Inorganic–organic hybrid; Cobalt; Channels structure; Antiferromagnetic

1. Introduction

Transition metal phosphates exhibiting open structures are being investigated for their many interesting properties and also for the possibility of investigating the interplay of structure, dimensionality and magnetism [1]. Recently, the pseudo pyramidal phosphite, H_3PO_3, group has been investigated with interest as a possible replacement for the traditional phosphate tetrahedra with great success. Thus, inorganic phosphite compounds with open-framework structures of different dimensionalities have been encountered for Zn [2–6], V [7–11], Cr [10,12], Mn [13], Fe [11,14–16], Co [17], Al [18], Ga [19], Be [20], and Mo [21]. Inorganic–organic hybrid compounds containing both oxalate and phosphate units have also been prepared [22–26]. Investigations on phosphite–oxalate framework on the other hand have been rare [27]. We have been interested in the study of mixed ligand frameworks, especially with phosphite and oxalate moieties. During the course of these investigations, we have now isolated a new cobalt phosphite–oxalate $[C_4N_2H_{12}][Co_4(HPO_3)_2(C_2O_4)_3]$, **I**, with three-dimensional structure. The structure of **I** closely resembles the phosphate–oxalate structure, $[C_4N_2H_{12}]_{0.5}[Co_2(HPO_4)(C_2O_4)_{1.5}]$, reported earlier [28]. In this paper, we describe the synthesis, structure and magnetic behavior of **I**.

2. Experimental

2.1. Synthesis and initial characterization

The cobalt phosphite–oxalate, $[C_4N_2H_{12}][Co_4(HPO_3)_2(C_2O_4)_3]$, **I,** was synthesized under hydrothermal

*Corresponding author. Fax: +91 80 2360 1310.
E-mail address: snatarajan@sscu.iisc.ernet.in (S. Natarajan).

0022-4596/$ - see front matter © 2005 Elsevier Inc. All rights reserved.
doi:10.1016/j.jssc.2005.05.020

conditions starting from cobalt (II) oxalate. In a typical synthesis, 0.285 g of CoC_2O_4 was dispersed in 7 mL deionized water. To this, 0.318 g of H_3PO_3 and 0.334 g of piperazine were added and the mixture was homogenized for 30 min at room temperature. The final mixture with the composition, $1.0CoC_2O_4$: $2.0H_3PO_3$: 2.0Piperazine: $200H_2O$, was transferred in to a 23-mL acid digestion bomb and heated at 150 °C for 96 h followed by at 180 °C for 24 h. The resulting product, contained large quantities of pink-colored cube-like single crystals only. The product was filtered under vacuum and washed with copious amount of deionized water, and dried at ambient conditions. The yield of the product was ~80% based on Co. The initial and final pH of the reaction mixture was ~4.

The initial characterizations were carried out using powder X-ray diffraction (XRD), thermogravimetric analysis (TGA) and infrared (IR) measurements. The powder XRD patterns were recorded on crushed single crystal in the 2θ range 5–50° using Cu$K\alpha$ radiation (Philips, X'pert Pro). The XRD pattern was entirely consistent with the structures determined using the single-crystal XRD (Fig. 1). A least squares fit of the powder XRD lines (Cu$K\alpha$) using the hkl indices generated from single-crystal X-ray data, gave the cell parameters $a = 7.639(2)$, $b = 7.523(2)$, $c = 17.792(4)$ Å and $\beta = 97.20(2)°$, which is in good agreement with that determined by single-crystal XRD.

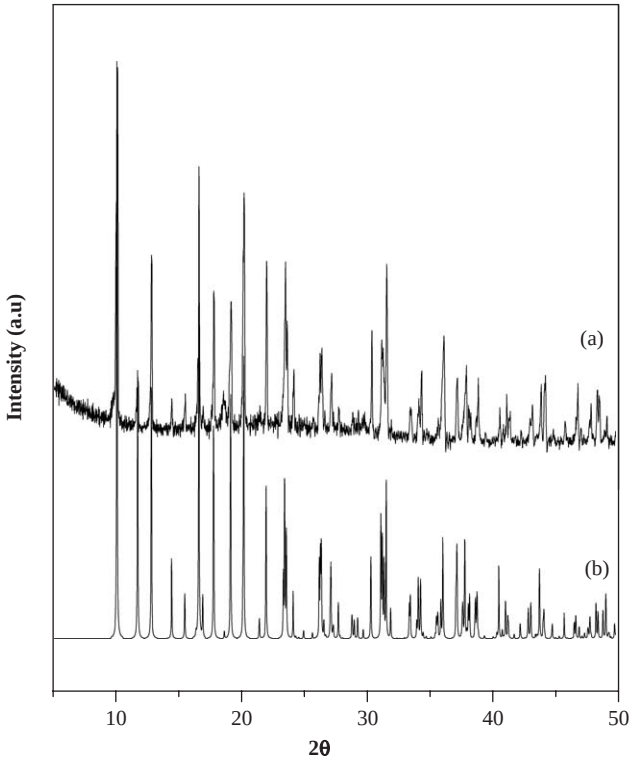

Fig. 1. Powder X-ray diffraction pattern (Cu$K\alpha$) for $[C_4N_2H_{12}][Co_4(HPO_3)_2(C_2O_4)_3]$, **I**, (a) experimental and (b) simulated.

TGA of the title compound, in an atmosphere of flowing air (flow rate = 50 mL/min) was carried out in the temperature range 25–750 °C (heating rate = 5 °C/min) (Fig. 2). The studies show a small initial weight loss at 125 °C followed by a broad weight loss from 280 to 500 °C. The small weight loss at 125 °C may be due to some absorbed water. A rapid weight loss of 40.1%, between the 280 and 500 °C corresponds to the deprotanation and volatilization of the organic amine and the decomposition of the oxalate to CO_2(g). The final decomposition products, identified by powder XRD, were $Co_3^{II}(P^VO_4)_2$ (JCPDS: 13-0503) and CoO (JCPDS: 43-1004). The calculated weight loss due to the decomposition of the organic amine and the oxalate moiety is 45.14% but the observed weight loss was 40.1% only. This anomalous result can be explained by considering the oxidation of P(III) to P(V) under the experimental conditions. The calculated weight gain due to oxidation of P(III) to P(V) is 4.1%. So total weight loss would be 44.2% (40.1 + 4.1), which is closer to the calculated weight loss (45.2%). The total weight loss equilibrium can be understood as follows:

$$[Co_4^{II}(HPO_3)_2(C_2O_4)_3]^{2-} + 2H^+ + 2.5O_2 = [Co_3^{II}(P^VO_4)_2]\ (s) + Co^{II}O\ (s) + 6CO_2(g)\uparrow + 2H_2O(g)\uparrow.$$

The other way to explain the TGA results is to compare the formula weights of **I** with that of the products. Thus, [formula weight of **I**−(formula weights

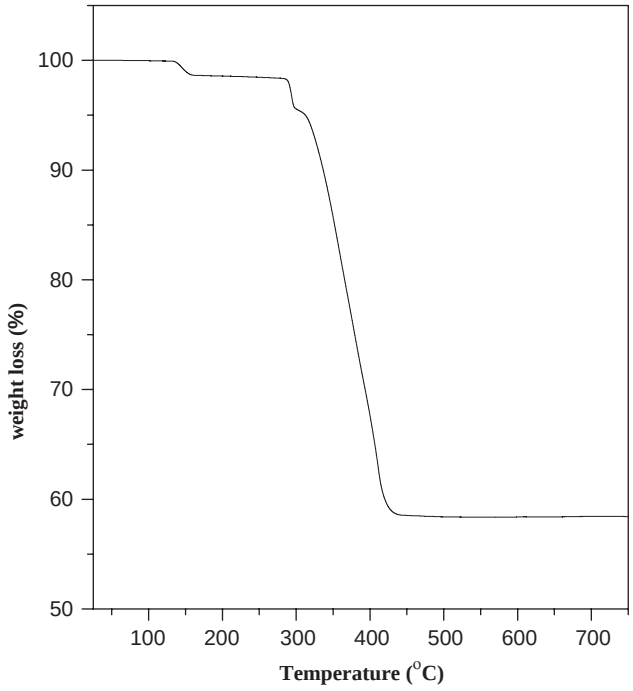

Fig. 2. TGA curve for $[C_4N_2H_{12}][Co_4(HPO_3)_2(C_2O_4)_3]$, **I**, showing the weight loss.

of $Co_3(PO_4)_2 + CoO$)/formula weight of **I**], gives a value of 40.9% which is the observed weight loss.

IR spectroscopic studies were carried out in the range 400–4000 cm^{-1} using KBr pellet method (Bruker IFS-66v). The IR spectrum of $[C_4N_2H_{12}][Co_4(HPO_3)_2(C_2O_4)_3]$, **I**, shows the characteristic bands of the protonated piperazine molecule, HPO_3 unit and C_2O_4 moieties. The observed IR bands are: $\nu(H_2O) = 3418\ cm^{-1}$, $\nu(NH) = 3370\ cm^{-1}$, $\nu(CH) = 3112\ cm^{-1}$, $\nu(PH) = 2376\ cm^{-1}$, $\nu(CC) = 1654\ cm^{-1}$, $\delta(CH) = 1459\ cm^{-1}$, $\delta(CO) = 1356\ cm^{-1}$, $\delta_{as}(PO_3) = 1136\ cm^{-1}$, $\delta(HP) = 981\ cm^{-1}$, $\delta_s(PO_3) = 582\ cm^{-1}$, $\delta_{as}(PO_3) = 491\ cm^{-1}$.

The temperature variation of the magnetic susceptibility studies has been carried out on powdered single crystals in the range 10–300 K using a Series 300 Lewis Coil Faraday Force magnetometer (Model C).

2.2. Single-crystal structure determination

A suitable pink-colored single crystal was carefully selected under a polarizing microscope and glued to a thin glass fiber with cyanoacrylate (superglue) adhesive. The single-crystal diffraction data were collected on a Bruker AXS Smart Apex CCD diffractometer at 293(2) K. The X-ray generator was operated at 50 kV and 35 mA using Mo$K\alpha$ ($\lambda = 0.71073$ Å) radiation. Data were collected with ω scan width of 0.3°. A total 606 frames were collected in three different settings of φ (0°, 90°, 180°) keeping the sample-to-detector distance fixed at 6.03 cm and the detector position (2θ) fixed at −25°. Pertinent experimental details for the structure determination of **I** are presented in Tables 1 and 2.

Table 1
Crystal data and structure refinement parameters for $[C_4N_2H_{12}][Co_4(HPO_3)_2(C_2O_4)_3]$, **I**

Empirical formula	$C_{10}H_{14}N_2O_{18}P_2Co_4$
Formula weight	747.894
Crystal system	Monoclinic
Space group	$P2_1/c$ (No. 14)
a (Å)	7.614 (15)
b (Å)	7.514 (14)
c (Å)	17.750 (3)
β (deg)	97.351 (3)
Volume (Å^3)	1007.30 (3)
Z	2
T (K)	293(2)
ρ_{calc} (g cm^{-3})	2.466
μ (mm^{-1})	3.496
θ range (deg)	2.31–25.99°
λ (Mo $K\alpha$) (Å)	0.71073
R indexes [$I > 2\sigma(I)$]	$R_1 = 0.0310$, w$R_2 = 0.0807$
R (all data)	$R_1 = 0.0293$, w$R_2 = 0.0798$

$R_1 = \sum ||F_o| - |F_c|| / \sum |F_o|$; w$R_2 = \{\sum[w(F_o^2 - F_c^2)] / \sum[w(F_o^2)^2]\}^{1/2}$.
$w = 1/[\rho^2(F_o)^2 + (aP)^2 + bP]$.
$P = [\max(F_o, O) + 2(F_c)^2]/3$, where $a = 0.0448$ and $b = 2.6507$.

Table 2
Final atomic coordinates [$\times 10^4$] and equivalent isotropic displacement parameters [Å $\times 10^3$] for $[C_4N_2H_{12}][Co_4(HPO_3)_2(C_2O_4)_3]$, **I**

Atom	x	y	z	$U_{(eq)}$[a]
Co(1)	3793(1)	4426(1)	1381(1)	15(1)
Co(2)	7253(1)	6802(1)	1934(1)	16(1)
P(1)	5510(1)	676(1)	1883(1)	14(1)
O(1)	4282(3)	1803(3)	1337(1)	19(1)
O(2)	2088(3)	6539(3)	1222(1)	24(1)
O(3)	5988(3)	5342(3)	931(1)	18(1)
O(4)	5240(3)	5449(3)	2357(1)	19(1)
O(5)	2975(3)	4099(3)	168(1)	23(1)
O(6)	1628(3)	3566(3)	2022(1)	19(1)
O(7)	5926(3)	8929(3)	1534(1)	24(1)
O(8)	9430(3)	7483(3)	1411(1)	20(1)
O(9)	8993(3)	4651(3)	2261(2)	25(1)
C(1)	5886(4)	5368(4)	213(18)	15(1)
C(2)	10401(4)	4711(4)	1972(2)	16(1)
C(3)	10667(4)	6383(4)	1493(2)	17(1)
C(10)	9580(6)	1440(6)	485(2)	37(1)
N(1)	8148(6)	381(6)	6(3)	55(1)
C(11)	11160(5)	324(5)	679(2)	24(1)

[a] $U_{(eq)}$ is defined as one third of the trace of the orthogonalized u_{ij} tensor.

The data were reduced using SAINTPLUS [29], and an empirical absorption correction was applied using the package SADABS program [30]. XPREP [29] was used to determine the space group. The crystal structure was solved and refined by using SHELXL97 present in the program suit WinGx (Version 1.63.04a) [31]. The hydrogen atom in the P–H group and all other hydrogen positions were initially located in the difference Fourier map and for the final refinement the hydrogen atoms were placed in geometrically ideal positions and refined using the riding mode. The last cycles of refinements included atomic positions, anisotropic thermal parameters for all the non-hydrogen atoms, isotropic thermal parameters for all the hydrogen atoms. Full-matrix-least-squares structure refinement against $|F^2|$ was carried out using the SHELXL package of programs [31]. Selected bond distances and bond angles for **I** are presented in Table 3.

3. Results and discussion

The asymmetric unit of **I** consists of 18 non-hydrogens atoms, of which two Co and one P atoms are crystallographically independent (Fig. 3). The cobalt atoms have octahedral coordination with respect to the oxygen atoms with an average Co–O bond distances of 2.113 Å. Both the cobalt atoms make two Co–O–P and four Co–O–C bonds with an average angle of 128.83° and 119.15°, respectively. The P atoms, on other hand make only three P–O–Co bonds and possess one P–H bond. The P–O bond distance have an average value of 1.52 Å. Out of nine oxygen atoms in the asymmetric

Table 3
Selected bond distances and angles in $[C_4N_2H_{12}][Co_4(HPO_3)_2(C_2O_4)_3]$, **I**

Bond	Distances, (Å)	Bond	Distances, (Å)
Co(1)–O (1) [0.4233]	2.010(2)	Co(2)–O (7) [0.4664]	1.974(2)
Co(1)–O(2) [0.3830]	2.047(2)	Co(2)–O(8) [0.3649]	2.065(2)
Co(1)–O(3) [0.3698]	2.060(2)	Co(2)–O(9) [0.3119]	2.123(2)
Co(1)–O(4) [0.3532]	2.077(2)	Co(2)–O(6) #1 [0.1698]	2.348(2)
Co(1)–O(5) [0.2688]	2.178(2)	**∑(Co(2)–O)**	**1.9346**
Co(1)–O(6) [0.2426]	2.216(2)	P(1)–O(7) #2	1.503(2)
∑(Co(1)–O)	**2.0407**	P(1)–O(1)	1.517(2)
Co(2)–O(3) [0.2506]	2.204(2)	P(1)–O(4) #3	1.541(2)
Co(2)–O(4) [0.3908]	2.059(2)	P(1)–H(10)	1.32
Moiety	Angle (°)	Moiety	Angle (°)
O(1)–Co(1)–O(2)	150.77(10)	O(4)–Co(2)–O(9)	89.56(9)
O(1)–Co(1)–O(3)	98.56(10)	O(7)–Co(2)–O(8)	92.34(10)
O(1)–Co(1)–O(4)	108.32(9)	O(7)–Co(2)–O(9)	170.93(10)
O(1)–Co(1)–O(5)	83.18(10)	O(8)–Co(2)–O(9)	78.62(9)
O(1)–Co(1)–O(6)	83.56(9)	Co(1)–O(1)–P(1)	128.65(14)
O(2)–Co(1)–O(3)	102.68(9)	Co(1)–O(3)–Co(2)	98.41(9)
O(2)–Co(1)–O(4)	95.01(10)	Co(1)–O(3)–C(1)	116.51(2)
O(2)–Co(1)–O(5)	81.70(10)	Co(2)–O(3)–C(1)	140.21(2)
O(2)–Co(1)–O(6)	78.26(9)	Co(1)–O(4)–Co(2)	102.66(1)
O(3)–Co(1)–O(4)	80.16(9)	Co(2)–O(8)–C(3)	114.89(2)
O(3)–Co(1)–O(5)	78.37(9)	Co(2)–O(9)–C(2)	113.52(2)
O(3)–Co(1)–O(6)	171.85(9)	O(9)–C(2)–C(3)	115.85(28)
O(4)–Co(1)–O(5)	156.96(9)	O(8)–C(3)–C(2)	116.93(28)
O(4)–Co(1)–O(6)	91.70(9)	P(1)–O(1)–Co(1)	128.65(14)
O(5)–Co(1)–O(6)	109.74(9)	P(1) #1–O(4)–Co(1)	123.68(13)
O(3)–Co(2)–O(4)	77.26(9)	P(1) #1–O(4)–Co(2)	129.87(14)
O(3)–Co(2)–O(7)	87.81(9)	P(1) #4–O(7)–Co(2)	133.15(15)
O(3)–Co(2)–O(8)	93.08(9)	C(1)–O(3)–Co(1)	116.5(2)
O(3)–Co(2)–O(9)	92.00(9)	C(1)–O(5)–Co(1)	111.9(2)
O(4)–Co(2)–O(7)	99.23(1)	C(2)–O(6)–Co(1)	110.9(2)
O(4)–Co(2)–O(8)	164.55(9)	C(2)–O(6)–Co(2)	129.1(2)

Values in brackets are the bond valences. Their sum VB appears in bold type at the end of the list of the distances around every cations. Symmetry transformations used to generate equivalent atoms: #1 $-x+1, y+1/2, -z+1/2$; #2 $x, y-1, z$; #3 $-x+1, y-1/2, -z+1/2$; #4 $x-1, y, z$.

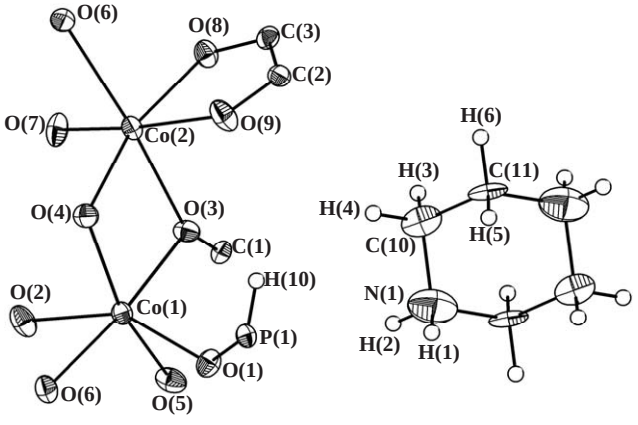

Fig. 3. ORTEP plot of **I**, showing the asymmetric unit. Thermal ellipsoids are given at 50% probability.

unit, three oxygen are three-coordinated (33%). Thus O(3) connects Co(1), Co(2) and C(1) atoms, O(4) connects Co(1), Co(2) and P(1) and O(6) connects Co(1), Co(2) and C(2) atoms.

The framework structure of $[C_4N_2H_{12}][Co_4(HPO_3)_2(C_2O_4)_3]$, **I**, comprises a network of CoO_6 octahedra, HPO_3 pseudo pyramidal and the oxalate groups. The $Co(1)O_6$ and $Co(2)O_6$ octahedra are connected by the two three-coordinated oxygen atoms [O(3) and O(4)] forming an edge-shared dimer, $[Co_2O_{10}]$. The dimers are connected via another three-coordinated oxygen [O(6)], forming an infinite one-dimensional Co–O–Co chains. The HPO_3 groups are grafted onto these chains (Fig. 4a). The cobalt phosphite chains are connected via an oxalate bridge to give rise to a two-dimensional hybrid structure. The hybrid two-dimensional cobalt phosphite–oxalate sheets are further connected by another oxalate in a direction perpendicular to the plane of the layer completing the three-dimensional connectivity. Thus, there are two types of oxalate units in the phosphite–oxalate, one connecting the chains within the plane forming hybrid layers and the other connecting the hybrid layers (Fig. 4b). This type of connectivity has been observed previously in the three-dimensional structure of zinc oxalate [32] and cobalt phosphate–oxalate [28]. The connectivity gives rise to one-dimensional channels of width 7.1×6.7 Å (longest atom–atom contact distances not including the van der Waals radii). The piperazinium cations occupy these channels.

An alternate description of the structure of **I** could be a simple Co^{II} oxalate structure formed by *in-plane* and *out-of-plane* connectivities of the oxalate units, templated by the piperazine molecules. This visualization and description is possible because the phosphite groups does not contribute to the connectivity of the overall structure and appear to decorate only the Co–O–Co chains in **I** by linking with three Co centers through the oxygen atoms as shown in Fig. 4a. This situation may be contrasted with that of the phosphate–oxalate structure of cobalt [28]. Co^{II} oxalate templated by organic amine molecules exhibiting three-dimensional structure has not been described in the literature, though such a structure has been realized in a zinc oxalate containing both the *in-plane* and *out-of-plane* oxalate linkages [32]. It is likely that the combined presence of the oxalate and the P^{3+} ions might have facilitated the formation of this unusual feature in **I**.

The cobalt phosphite–oxalate structure has close similarity with the cobalt phosphate–oxalate structure $[C_4N_2H_{12}]_{0..5}[Co_2(HPO_4)(C_2O_4)_{1.5}]$ [28]. In **I**, two CoO_6 octahedra are connected forming a Co_2O_{10} edge-shared dimer and in the phosphate–oxalate structure CoO_6 and CoO_5 polyhedral units are connected to form Co_2O_9 dimers. In addition, the Co_2O_9 dimers are isolated and are joined by PO_4 groups. In **I**, Co_2O_{10} dimers are

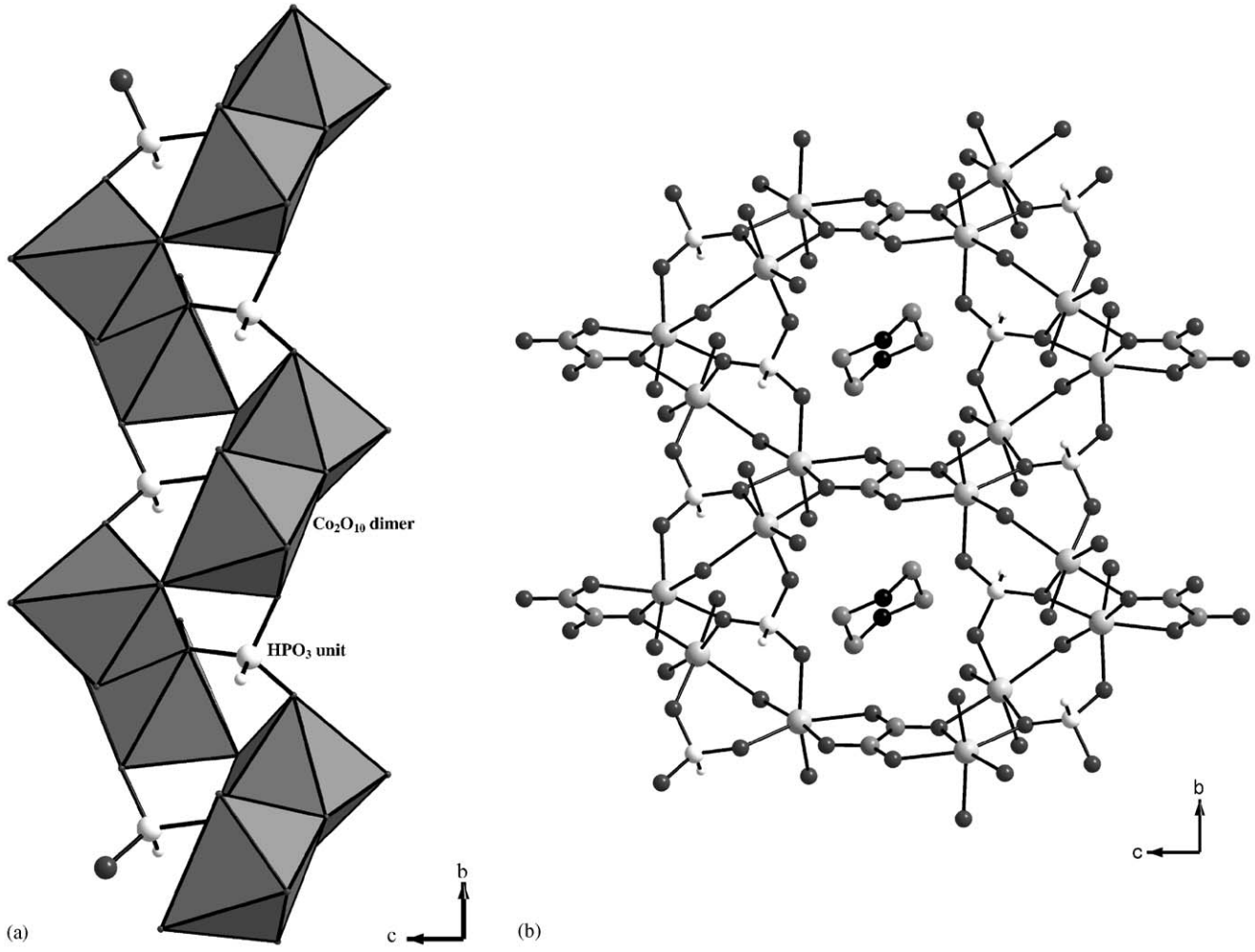

Fig. 4. (a) Structure of $[C_4N_2H_{12}][Co_4(HPO_3)_2(C_2O_4)_3]$, **I**, showing the $[Co_2O_{10}]$ dimers and its connectivity. Note that the dimmers are connected through the oxygen atoms forming infinite Co–O–Co chains (see text). The phosphite groups decorate the Co–O–Co chains. (b) Structure of **I** in the *bc* plane showing the channels. Hydrogen atoms of the amine molecule are not shown.

connected by oxygen atoms forming infinite one-dimensional Co–O–Co chains. Both the compounds have the piperazine molecule in the middle of the channels. Another way to describe the structure of **I** is to describe as a simple cobalt oxalate structure.

The presence of Co–O–Co infinite one-dimensional chain in **I** can impart interesting magnetic properties, with the predictable existence of magnetic couplings between the d^7 centers. Temperature variation of the magnetic susceptibility of $[C_4N_2H_{12}][Co_4(HPO_3)_2(C_2O_4)_3]$, **I,** was carried out using a Faraday Force magnetometer under 0.2 T magnetic field from 10–300 K (Fig. 5). The molar magnetic susceptibility increases as the temperature is decreased and reaches a sharp maximum at ~22 K. The linear fit of the magnetic data above 150 K indicates a Curie–Weiss behavior ($C = 8.133$ emu/mol and $\theta p = -40$ K).

A careful examination of the structure shows that the $[Co_2O_{10}]$ dimers are connected continuously forming a chain and the chains are connected via the oxalate units.

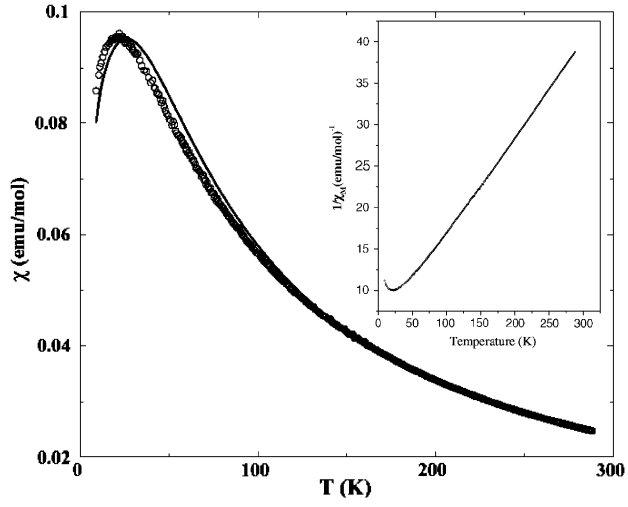

Fig. 5. Temperature dependence of magnetic susceptibility for $[C_4N_2H_{12}][Co_4(HPO_3)_2(C_2O_4)_3]$. Solid line is the exponential fit to the experimental data (see text). Inset shows the inverse of the susceptibility as a function of temperature.

According to Goodenough if the d^7–d^7 exchange with an angle of 180° the interactions are always antiferromagnetic and the 90° ones can either be antiferromagnetic or ferromagnetic [33]. The angle Co(1)–O(3)–Co(2) is 98.41°, Co(2)–O(4)–Co(1) is 102.66° and Co(1)–O(6)–Co(2) is 110.58°, which are closer to the 90° interaction range. This indicates that the exchange interactions through the Co^{2+}–O–Co^{2+} pathway could be moderately strong. The value of θp (−40 K), obtained from the Curie–Weiss fit also indicates moderate antiferromagnetic interactions. Short-range ordering, in general, are associated with the low-dimensional antiferromagnetic systems [34]. Since the structure possess the Co^{II} octahedral connected through their edges forming a dimer, to understand the magnetic behavior in **I**, we have employed a model commonly used in dimeric complexes. Thus, in the Heisenberg model for two $S = \frac{3}{2}$ spins (dimer, d^7 system), the magnetic energy levels can be written as $E_S = J/2[S(S+1) - 15/2]$ with S values 0,1,2, and 3 [35]. The magnetic susceptibility can be defined as $\chi T = \langle M^2\rangle - \langle M\rangle^2$, where $[\langle M^2\rangle - \langle M\rangle^2]$ is the fluctuation in the magnetization, M. For antiferromagnetic system $\langle M^2\rangle$ vanishes when the field becomes zero. The magnetic susceptibility for the d^7 dimer (Co^{II}) can be written as $\chi_{\text{dimer}} = g^2\mu B^2/K_B T[\sum_S\{S(S+1)\exp(E_S/K_B T)\}/\sum_S \exp(E_S/K_B T)]$, $S = 0, 1, 2,$ and 3. We have fitted this dimer susceptibility with the experimental χ_m, by varying the exchange constant, J, and the Lande factor, g. The best fit was obtained with $g = 2.01$ and $J = -12$ K. This type of magnetic behavior has been observed in the iron arsenate structure and in the binuclear Co^{II} complexes [36,37]. We have calculated the effective magnetic moment from the $\chi_{\text{dimer}}T$ formula by using the fitted values of g and J. The calculated room temperature magnetic moment (3.7 μB) compares well with the spin only value of Co^{II} in the high spin state (3.8 μB). The observed effective magnetic moment (μ_{eff}) also compares well with the presence of cobalt in the +2 state. The result showed that the dimers are coupled antiferromagnetically with in the chain and in a super exchange way between the chains through the oxalates. Similar magnetic behavior has been encountered in the iron phosphate–oxalate [22–24] and cobalt carboxylate [38,39] and in the cobalt phosphate–oxalate [28].

In summary, the synthesis, structure and magnetic properties of an inorganic–organic hybrid cobalt phosphite–oxalate has been accomplished. The presence of Co_2O_{10} dimers and the resulting Co–O–Co one-dimensional chains are noteworthy structural features. The compound orders antiferromagnetically at low temperature. The presence of the pseudo tetrahedral HPO_3 unit along with the rigid linear $[C_2O_4]$ in **I** indicates that it is profitable to explore this area further as many new compounds with novel structures are likely to be discovered. We are currently pursuing this theme.

Acknowledgments

S.M gratefully acknowledges University Grant Commission (UGC), Government of India, for the award of a research fellowship. S.N. thanks the Department of Science and Technology (DST) and the Council of Scientific and Industrial Research (CSIR), Government of India, for the award of research grants. We thank DST-IRHRA, India for the CCD facility. The authors thank Professor Swapan K. Pati, JNCASR, for his help with the modeling of the magnetic behavior.

Appendix A. Supplementary Information

The online version of this article contains additional supplementary data. Please visit doi:10.1016/j.jssc.2005.05.020.

References

[1] N. Guillo, Q. Gao, P.M. Foster, J.-S. Chang, M. Nogues, S.-E. Park, G. Ferey, A.K. Cheetham, Angew. Chem. Int. Ed. 40 (2001) 2831.
[2] W.S. Fu, Z. Shi, G.N. Li, D. Zhang, W.J. Dong, X.B. Chen, S.H. Feng, Solid State Sci. 6 (2004) 225.
[3] J. Liang, Y. Wang, J.H. Yu, Y. Li, R.R. Xu, Chem. Commun. (2003) 882.
[4] W.T.A. Harrison, M.L.F. Phillips, J. Stranchfield, T.M. Nenoff, Inorg. Chem. 40 (2001) 895.
[5] J.A. Rodgers, W.T.A. Harrison, Chem. Commun. (2000) 2385.
[6] Y. Wang, J.H. Yu, Y. Du, Z. Shi, Y.C. Zou, R.R. Xu, J.Chem. Soc. Dalton Trans. (2002) 4060.
[7] Z. Shi, D. Zhang, G.H. Li, L. Wang, X.Y. Lu, J. Hua, S.H. Feng, J. Solid State Chem. 172 (2003) 464.
[8] W.T.A. Harrison, Solid State Sci. 5 (2003) 2357.
[9] Z. Shi, G.H. Li, D. Zhang, J. Hua, S.H. Feng, Inorg. Chem. 42 (2003) 2357.
[10] S. Fernandez, J.L. Mesa, J.L. Pizarro, L. Lezama, M.I. Arriortua, T. Rojo, Chem. Mater. 15 (2003) 1204.
[11] S. Fernandez, J.L. Mesa, J.L. Pizarro, L. Lezama, M.I. Arriortua, T. Rojo, Chem. Mater. 14 (2002) 2300.
[12] S. Fernandez, J.L. Mesa, J.L. Pizarro, L. Lezama, M.I. Arriortua, T. Rojo, Angew. Chem. Int. Ed. 41 (2002) 3683.
[13] S. Fernandez, J.L. Mesa, J.L. Pizarro, L. Lezama, M.I. Arriortua, R. Olazcuaga, T. Rojo, Chem. Mater. 12 (2000) 2092.
[14] S. Fernandez-Armas, J.L. Mesa, J.L. Pizarro, J.S. Garitanandia, M.I. Arriortua, T. Rojo, Angew. Chem. Int. Ed. 43 (2004) 977.
[15] U.C. Chung, J.L. Mesa, J.L. Pizarro, L. Lezama, J.S. Garitaonandia, J.P. Chapman, M.I. Arriotua, J. Solid State Chem. 177 (2004) 2705.
[16] S. Mandal, S.K. Pati, M.A. Green, S. Natarajan, Chem. Mater. 17 (2005) 638–643.
[17] S. Fernandez, J.L. Mesa, J.L. Pizarro, L. Lezama, M.I. Arriortua, T. Rojo, Int. J. Inorg. Mater. 3 (2001) 331.
[18] H.G. Harvey, J. Hu, M.P. Attfield, Chem. Mater. 15 (2003) 179.
[19] S. Fernandez-Armas, J.L. Mesa, J.L. Pizarro, L. Lezama, M.I. Arriortua, T. Rojo, J. Solid State Chem. 177 (2004) 297.
[20] W.S. Fu, L. Wang, Z. Shi, G.H. Li, X.B. Chen, Z.M. Dai, L. Yang, S.H. Feng, Cryst. Growth Des. 4 (2004) 297.
[21] D.G. Lyxell, D. Bostrom, M. Hashimoto, L. Petterson, Acta Chim. Scand. 52 (1998) 425.

[22] A. Choudhury, S. Natarajan, C.N.R. Rao, Chem. Mater. 11 (1999) 2316.
[23] A. Choudhury, S. Natarajan, C.N.R. Rao, J. Solid State Chem. 146 (1999) 538.
[24] A. Choudhury, S. Natarajan, J. Mater. Chem. 9 (1999) 3113.
[25] Y.-C. Jiang, S.-L. Wang, K.H. Lii, N. Nguyen, A. Ducouret, Chem. Mater. 15 (2003) 1633.
[26] Y.-C. Jiang, S.-L. Wang, S.-F. Lee, K.H. Lii, Inorg. Chem. 42 (2003) 6154.
[27] S. Mandal, S.K. Pati, M.A. Green, S. Natarajan, Chem. Mater. 17 (2005) 2912.
[28] A. Choudhury, S. Natarajan, Solid State Sci. 2 (2000) 365.
[29] SMART (V 5.628). SAINT (V 6.45a), XPREP, SHELXTL, Bruker AXS Inc., Madison, WI, 2004.
[30] G.M. Sheldrick, SADABS Siemens Area Correction Absorption Correction Program, University of Göttingen, Göttingen, Germany, 1994.
[31] G.M. Sheldrick, SHELXL-97 Program for Crystal Structure Solution and Refinement, University of Göttingen, Göttingen, Germany, 1997.
[32] R. Vaidhyanathan, S. Natarajan, C.N.R. Rao, Chem. Mater. 11 (1999) 3636.
[33] J.B. Goodenough, Magnetism and Chemical Bonds, Wiley-Interscience, New York, 1963.
[34] R. Chitra, S.K. Pati, H.R. Krishnamurthy, D. Sen, S. Ramasesha, Phys. Rev. B 52 (1995) 6582.
[35] R.L. Carlin, Magnetochemistry, Springer, Berlin, 1986.
[36] S. Chakrabarti, S.K. Pati, M.A. Green, S. Natarajan, Eur. J. Inorg. Chem. (2003) 3820–3825.
[37] B. Chiari, A. Cinti, O. Crispu, F. Demartin, A. Pasini, O. Piovesana, J. Chem. Soc., Dalton Trans. (2001) 3611–3616.
[38] C. Livage, C. Eagger, M. Nogues, G. Ferey, J. Mater. Chem. 8 (1998) 2743.
[39] C. Livage, C. Egger, G. Ferey, Chem. Mater. 11 (1999) 1546.